Stochastic study of a non-linear self-excited system with friction

Emmanuelle Sarrouy, Olivier Dessombz, Jean-Jacques Sinou

Stochastic study of a non-linear self-excited system with friction

E. Sarrouy[a,*], O. Dessombz[a], J-J. Sinou[a]

[a] *Ecole Centrale de Lyon, Laboratoire de Tribologie et Dynamique des Systèmes (UMR CNRS 5513), 36 avenue Guy de Collongue, 69134 Ecully Cedex, France*

Abstract

This paper proposes two methods based on the Polynomial Chaos to carry out the stochastic study of a self-excited non-linear system with friction which is commonly used to represent brake-squeal phenomenon. These methods are illustrated using three uncertain configurations and validated using comparison with Monte Carlo simulation results. First, the stability of the static equilibrium point is examined by computing stochastic eigenvalues. Then, for unstable ranges of the equilibrium point, a constrained harmonic balance method is developed to determine subsequent limit cycles in the deterministic case; it is then adapted to the stochastic case. This demonstrates the effectiveness of the methods to fit complex eigenmodes as well as limit cycles dispersion with a good accuracy.

Keywords: friction, stochastic, polynomial chaos, eigenvalue problem, limit cycles

*Corresponding author. Tel: +33 472186464/Fax:+33 472189144

Email addresses: emmanuelle.sarrouy@(ec-lyon.fr,gmail.com) (E. Sarrouy), olivier.dessombz@ec-lyon.fr (O. Dessombz), jean-jacques.sinou@ec-lyon.fr (J-J. Sinou)

1. Introduction

This work follows the study conducted in (Sinou and Jézéquel, 2007b) which investigated the influence of damping and friction coefficient on the stability of the equilibrium point using an analytical deterministic criterion. The main results of this study are recalled in Section 2.1. Our objective is to propose a stochastic approach for such a system and to demonstrate the ability of the proposed method to handle systems with friction in a more general view. Brake systems are indeed hard to characterize accurately because of the high variability of operating conditions (Ibrahim, 1994). A stochastic approach seems then highly adequate for design of robust products. If Monte Carlo (MC) simulations can be carried out for small models, it is way too expensive for larger systems such as finite element models used in industrial context. Moreover, brake squeal arises as the static equilibrium becomes unstable (Kinkaid et al., 2003). In this case, the system - being non-linear - converges toward limit cycles whose amplitude and frequency are unknown: these systems are part of the self-excited systems family. Characterization of these limit cycles is then an important point to be taken care of.

The method proposed herein, based on the expansion of stochastic elements on the Polynomial Chaos, is much less expensive than MC simulations when it comes to larger systems and does not share convergence radius problems as methods relying on Taylor series do (Ghanem and Spanos, 2003). Some recent work uses Polynomial Chaos expansion and derivatives such as Multi-Element generalized Polynomial Chaos (MEgPC) (Wan and Karniadakis, 2005) to demonstrate stability of equilibria of stochastic systems using the Lyapunov function (Fisher and Bhattacharya, 2008; Nechak et al., 2011) or

to compute limit cycles in the time domain (Nechak et al., 2012) when the equilibrium loses stability. Recent papers propose evaluation of Hopf bifurcation point (when stability changes) using MEgPC for a system with dry friction when one parameter (the friction coefficient) varies but does not investigate the non-linear effects in the unstable range (see (Nechak et al., 2013) for a 2-dofs system and (Sarrouy et al., 2013) for a finite element model of a brake).

Our first objective is to show that using a proper decomposition of eigenmodes, Polynomial Chaos provides accurate results on eigenvalues dispersion resulting from one or more uncertain parameters and hence on the stability of equilibria for a system undergoing multiple uncertainty sources. The second point of this paper addresses the dispersion of limit cycles that occur in the unstable ranges which are responsible for brake squeal. To this end, a constrained harmonic balance method is proposed. This modified harmonic balance method overcomes the problem of dealing with an unknown cycle period and long term integration problems that arise when using a time integration scheme as in (Nechak et al., 2012). The proposed method suits both deterministic and stochastic cases.

The paper is composed as follows: Section 2 first exposes the model and its equations along with main results from previous deterministic study. The three uncertain configurations that will be numerically processed are then detailed. Section 3 is devoted to theoretical discussion. First, computation of eigenmodes using a Polynomial Chaos expansion is explained. Then, the method for computing the limit cycles is exposed in the deterministic context and adapted to the stochastic approach. Finally, numerical results for

the three uncertain cases illustrate efficiency of the methods and physical phenomena are analysed.

2. System deterministic study

A simple system similar to the one studied in (Sinou and Jézéquel, 2007b) is considered. This kind of phenomenological model was introduced by Hultén (1993) in order to study squeal vibration in drum brakes and is sufficient to investigate friction-induced vibrations. After a brief description, main deterministic results are recalled. Then, three uncertain configurations used as application material are described.

2.1. System description

The system considered is a simple mass linked to a moving band by two non-linear springs attached to plates ($k_1 + k_1^{\mathrm{nl}}$ and $k_2 + k_2^{\mathrm{nl}}$) in orthogonal directions . The friction coefficient at contact between the plates and the band is denoted μ. Damping is also introduced through c_1 and c_2 dashpots. A schematic is presented in Fig. 1. Such a low order model may not contain all the necessary information to provide fully reliable predictions as stated in recent studies (Butlin and Woodhouse, 2009, 2010). This non-linear 2 degrees of freedom model will nonetheless provide an acceptable method application support whose results may be compared to the conclusions of Sinou and Jézéquel (2007b). The proposed method could be applied without any modification to larger models.

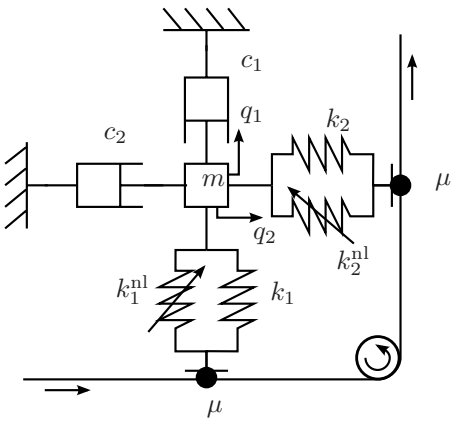

Figure 1: Mass with double rubbers: plan

Equations describing the system dynamic behaviour are:

$$\underbrace{\begin{bmatrix} 1 & 0 \\ 0 & 1 \end{bmatrix}}_{\mathbf{M}} \ddot{\mathbf{q}} + \underbrace{\begin{bmatrix} \eta_1\omega_{01} & 0 \\ 0 & \eta_2\omega_{02} \end{bmatrix}}_{\mathbf{D}} \dot{\mathbf{q}} + \underbrace{\begin{bmatrix} \omega_{01}^2 & -\mu\omega_{02}^2 \\ \mu\omega_{01}^2 & \omega_{02}^2 \end{bmatrix}}_{\mathbf{K}} \mathbf{q} + \underbrace{\begin{Bmatrix} \varphi_1 q_1^3 - \mu\varphi_2 q_2^3 \\ \mu\varphi_1 q_1^3 + \varphi_2 q_2^3 \end{Bmatrix}}_{\mathbf{f}_{\mathrm{nl}}(t,\mathbf{q},\dot{\mathbf{q}})} = \begin{Bmatrix} 0 \\ 0 \end{Bmatrix} \quad (1)$$

where $\omega_{0i} = \sqrt{k_i/m}$, $\eta_i = c_i/\sqrt{mk_i}$ and $\varphi_i = k_i^{\mathrm{nl}}/m$.

Base value set is $\omega_{01} = 2\pi \times 1000$ rad.s^{-1}, $\omega_{02} = 2\pi \times 600$ rad.s^{-1}, $\eta_1 = 0.06$, $\eta_2 = 0.02$, $\varphi_1 = 1 \cdot 10^{11}$ m^{-2}.s^{-2}, $\varphi_2 = 1 \cdot 10^{9}$ m^{-2}.s^{-2} and $\mu = 0.398$. $\mathbf{q}$ size will be denoted $n = 2$.

As demonstrated in (Sinou and Jézéquel, 2007b,a), this system has a null equilibrium ($\mathbf{q}^* = \mathbf{0}$ and $\dot{\mathbf{q}}^* = \mathbf{0}$) whose stability depends on the friction parameter μ. Stability is determined by real parts of eigenvalues of the

tangent system at equilibrium point:

$$\mathbf{M}\ddot{\mathbf{q}} + (\mathbf{D} + D_{\dot{\mathbf{q}}}\mathbf{f}_{\text{nl}}(t, \mathbf{q}^*, \dot{\mathbf{q}}^*))\,\dot{\mathbf{q}} + (\mathbf{K} + D_{\mathbf{q}}\mathbf{f}_{\text{nl}}(t, \mathbf{q}^*, \dot{\mathbf{q}}^*))\,\mathbf{q} = \mathbf{0} \tag{2}$$

where $D_{\mathbf{q}}\mathbf{f}_{\text{nl}}(t, \mathbf{q}^*, \dot{\mathbf{q}}^*)$ and $D_{\dot{\mathbf{q}}}\mathbf{f}_{\text{nl}}(t, \mathbf{q}^*, \dot{\mathbf{q}}^*)$ stand for derivatives of $\mathbf{f}_{\text{nl}}$ with respect to $\mathbf{q}$ and $\dot{\mathbf{q}}$ at equilibrium point $(\mathbf{q}^*, \dot{\mathbf{q}}^*)$. It turns out from $\mathbf{f}_{\text{nl}}$ expression that $D_{\dot{\mathbf{q}}}\mathbf{f}_{\text{nl}}(t, \mathbf{q}^*, \dot{\mathbf{q}}^*) = \mathbf{0}$ as the non-linear terms do not depend on $\dot{\mathbf{q}}$. Moreover, the equilibrium having null coordinates, $D_{\mathbf{q}}\mathbf{f}_{\text{nl}}(t, \mathbf{q}^*, \dot{\mathbf{q}}^*) = \mathbf{0}$ too. Then, the tangent system can be expressed in the following augmented form:

$$\underbrace{\begin{bmatrix} \mathbf{K} & \mathbf{0} \\ \mathbf{0} & \mathbf{M} \end{bmatrix}}_{\mathbf{B}} \dot{\mathbf{x}} - \underbrace{\begin{bmatrix} \mathbf{0} & \mathbf{K} \\ -\mathbf{K} & -\mathbf{D} \end{bmatrix}}_{\mathbf{A}} \mathbf{x} = \mathbf{0}, \ \mathbf{x} = \begin{Bmatrix} \mathbf{q} \\ \dot{\mathbf{q}} \end{Bmatrix} \tag{3}$$

The corresponding eigenvalue problem with a normalization condition which defines eigenvectors $\mathbf{u}_k$ uniquely is

$$\mathbf{A}\mathbf{u}_k = \lambda_k \mathbf{B}\mathbf{u}_k \text{ and } \mathbf{u}_k^T \mathbf{B}\mathbf{u}_k = 1, \quad 1 \leq k \leq 2n = 4 \tag{4}$$

Whenever one of the eigenvalue λ_k has a positive real part, the system is unstable.

For μ ranges for which instability occurs, the mode being unstable depends on the $(\eta_1\omega_1)/(\eta_2\omega_2)$ ratio. Non-linear springs lead to existence of limit cycles for these ranges, whose frequency is *a priori* unknown. Numerical determination of these limit cycles and of their frequencies is explained in Section 3.2.

2.2. Uncertain configurations

Three different uncertain configurations will be dealt with in Section 4, each of them having a different purpose. They are described below, including

numerical differences to the base value set previously stated.
Dispersion of parameters are expressed as functions of independent random variables ξ_i which follow a standard normal distribution. This is a classical distribution and matches the basic theoretical frame of Polynomial Chaos.

The first uncertain configuration considers dispersion on the friction coefficient μ. This will illustrate consequences of μ dispersion on the system stability and will be used to validate the method by comparing PC results to MC simulations. For this case, one will use

$$\mu(\xi) = \overline{\mu} + \Delta\mu\xi \tag{5}$$

with $\overline{\mu} = 0.398$ and $\Delta\mu = \frac{5}{100}\overline{\mu} = 0.0199$.
This dispersion impacts $\mathbf{K}$ matrix as well as the non-linear contribution $\mathbf{f}_{\text{nl}}$. The chosen set of values puts the system close to the stability limit.

The second configuration focuses on $(\eta_2\omega_{02})/(\eta_1\omega_{01})$ ratio action with regard to the mode becoming unstable. To this end, a μ value is chosen so as to ensure having an unstable static equilibrium. The ratio is varied by taking into account dispersion on η_2.

$$\eta_2(\xi) = \overline{\eta_2} + \Delta\eta_2\xi \tag{6}$$

with $\overline{\eta_2} = 0.034$ and $\Delta\eta_2 = \frac{14.7}{100}\overline{\eta_2} = 0.005$, that is a standard deviation equal to 14.7% of the mean value $\overline{\eta_2}$ for η_2. Moreover, $\eta_1 = 0.02$ and $\mu = 0.55$. The $(\eta_2\omega_{02})/(\eta_1\omega_{01})$ nominal ratio is then equal to 1.02.
Variation of η_2 implies variation of damping matrix $\mathbf{D}$ only.

Finally the two previous parameters undergo dispersion at the same time depending on two different random variables ξ_1 and ξ_2. This will prove that

both methods can handle configurations with multiple uncertain parameters.

$$\mu(\boldsymbol{\xi}) = \overline{\mu} + \Delta\mu\xi_1 \tag{7a}$$

$$\eta_2(\boldsymbol{\xi}) = \overline{\eta_2} + \Delta\eta_2\xi_2 \tag{7b}$$

with $\overline{\mu} = 0.56$, $\Delta\mu = \frac{1}{100}\overline{\mu} = 0.0056$, $\overline{\eta_2} = 0.0333$ and $\Delta\eta_2 = \frac{1}{100}\overline{\eta_2} = 0.000333$. Moreover, $\eta_1 = 0.02$ as in the previous case that is $(\eta_2\omega_{02})/(\eta_1\omega_{01}) = 1$. Theses variations affect $\mathbf{K}$ and $\mathbf{D}$ matrices as well as the non-linear forces $\mathbf{f}_{\text{nl}}$.

3. Theoretical discussion

Introducing uncertainty on some parameters modifies the dynamic equation (1) and uncertain quantities are to be added:

$$\left(\mathbf{M} + \tilde{\mathbf{M}}(\boldsymbol{\xi})\right)\ddot{\mathbf{q}} + \left(\mathbf{D} + \tilde{\mathbf{D}}(\boldsymbol{\xi})\right)\dot{\mathbf{q}} + \left(\mathbf{K} + \tilde{\mathbf{K}}(\boldsymbol{\xi})\right)\mathbf{q} + \tilde{\mathbf{f}}_{\text{nl}}(t, \dot{\mathbf{q}}, \dot{\mathbf{q}}; \boldsymbol{\xi}) = \mathbf{0} \tag{8}$$

where tilde quantities depend on a set of random variables $\boldsymbol{\xi}$ used to describe uncertainty. We assume that these variables follow a standard normal distribution.

The randomness of the inputs has consequences on eigenvalues. The method used to evaluate their dispersion is exposed in the next subsection. Furthermore, as stated in Section 2.1, limit cycles appear when equilibria become unstable. These cycles are also affected by dispersion of the inputs. Section 3.2 proposes a method to compute these limit cycles with unknown period in the deterministic case and its adaptation to the stochastic case.

3.1. Eigenvalue problem for equilibria

Using the same transformation that the one applied to (1) to get (4), the stochastic eigenvalue problem with a normalization condition is deduced

from (8):

$$\left(\mathbf{A}+\tilde{\mathbf{A}}(\boldsymbol{\xi})\right)\tilde{\mathbf{u}}_k=\tilde{\lambda}_k\left(\mathbf{B}+\tilde{\mathbf{B}}(\boldsymbol{\xi})\right)\tilde{\mathbf{u}}_k,\quad \tilde{\mathbf{u}}_k^T\left(\mathbf{B}+\tilde{\mathbf{B}}\right)\tilde{\mathbf{u}}_k=1,\quad 1\leq k\leq 2n \tag{9}$$

where tilde matrices are added to introduce uncertainty and $\tilde{\mathbf{u}}_k$ and $\tilde{\lambda}_k$ respectively denote stochastic eigenvectors and eigenvalues.

As stated in the introduction, the method at stake relies on the expansion of stochastic eigenmodes onto the Polynomial Chaos (PC). This expansion consists in decomposing uncertain quantities on a basis of Hermite multivariate polynomials denoted ψ_n as introduced by Ghanem and Spanos (2003). These polynomials are most appropriate for Gaussian stochastic processes. The computation of these polynomials and the appropriate scalar product are recalled in Appendix A.

Stochastic eigenvalues and eigenvectors of augmented system (9) are here decomposed on both the deterministic augmented eigenmodes and the polynomial chaos using complex weights:

$$\tilde{\lambda}_k(\boldsymbol{\xi})=\lambda_k\sum_{s=1}^{N}\left({}^{(k)}a_s+\mathbf{j}\,{}^{(k)}b_s\right)\psi_s(\boldsymbol{\xi}) \tag{10}$$

$$\tilde{\mathbf{u}}_k(\boldsymbol{\xi})=\sum_{p=1}^{P}\left({}^{(k)}\tilde{\gamma}_p(\boldsymbol{\xi})+\mathbf{j}\,{}^{(k)}\tilde{\mu}_p(\boldsymbol{\xi})\right)\mathbf{u}_p \tag{11}$$

with

$${}^{(k)}\tilde{\gamma}_p(\boldsymbol{\xi})=\sum_{n=1}^{N}{}^{(k)}\gamma_p^n\psi_n(\boldsymbol{\xi})\ \text{and}\ {}^{(k)}\tilde{\mu}_p(\boldsymbol{\xi})=\sum_{n=1}^{N}{}^{(k)}\mu_p^n\psi_n(\boldsymbol{\xi}) \tag{12}$$

giving

$$\tilde{\mathbf{u}}_k(\boldsymbol{\xi})=\sum_{p=1}^{P}\left(\sum_{n=1}^{N}\left({}^{(k)}\gamma_p^n+\mathbf{j}\,{}^{(k)}\mu_p^n\right)\psi_n(\boldsymbol{\xi})\right)\mathbf{u}_p \tag{13}$$

where the coefficients ${}^{(k)}\gamma_p^n$, ${}^{(k)}\mu_p^n$, ${}^{(k)}a_s$ and ${}^{(k)}b_s$ are real and $\mathbf{j}$ denotes the imaginary unit ($\mathbf{j}^2 = -1$). ψ_1 will conventionally denote the constant polynomial equal to 1; means of polynomials with index greater than or equal to 2 are then null.

This decomposition using P deterministic eigenvalues and eigenvectors is a generalization of what is proposed in (Dessombz, 2000; Dessombz et al., 1999). Using complex weights, real and imaginary parts of stochastic eigenvalues and eigenvectors can evolve independently. In this paper, all the deterministic modes are used for projection of stochastic eigenvectors, $P = 2n$.

Using this decomposition for eigenmodes, one also applies it to the stochastic matrices of Eq. (9). This new writing of matrices can be achieved by using a Karhunen-Loève decomposition or assuming them so regarding experimental results:

$$\tilde{\mathbf{A}} = \sum_{n=2}^{N_A} \mathbf{A}_n \psi_n(\boldsymbol{\xi}) \text{ and } \tilde{\mathbf{B}} = \sum_{n=2}^{N_B} \mathbf{B}_n \psi_n(\boldsymbol{\xi}) \tag{14}$$

Having $\psi_1(\boldsymbol{\xi}) = 1$, it is associated with the deterministic components $\mathbf{A}$ and $\mathbf{B}$ and only polynomials with zero mean are considered for the decomposition of these matrices.

To get the final system of equations that leads to the unknowns ${}^{(k)}\gamma_p^n$, ${}^{(k)}\mu_p^n$, ${}^{(k)}a_s$ and ${}^{(k)}b_s$ once solved, Eqs. (9) are projected onto the polynomial chaos basis $\psi_k(\boldsymbol{\xi})$, $1 \leq k \leq N$ using the dedicated scalar product defined in Appendix (A.5). During this step, one has to compute scalar products of the form $< \psi_{i_1} \dots \psi_{i_j}, \psi_n >$. Let us point out that these quantities can be evaluated and stored once for all, being reused for further studies and that many of them are null, implying simplification of the resulting set of equations. This is an advantage provided by the chosen intrusive approach

compared to non intrusive approaches which require the use of quadrature formula to evaluate the unknown coefficients. To overcome the problem of dealing with complex valued functions, real and imaginary parts of the subsequent equations are separated. This generates $2P(P+1)N$ non-linear (quadratic) equations, that is as many as unknowns. This set of equations can be solved through a general non-linear solver relying for example on the Levenberg-Marquardt scheme.

Once the PC expansion is obtained, stochastic indicators such as mean or standard deviation are computed by evaluating eigenmodes using their PC decomposition on a large MC sample.

3.2. Constrained HBM for limit cycles determination

3.2.1. Deterministic case

As recalled previously, the self-excited non-linear system tends to draw limit cycles when the static equilibrium is unstable. Coming from a mode coupling, these limit cycles have an unknown period. To determine their properties while avoiding a direct time-integration process, a well-known method is the harmonic balance method (HBM) which consists in a Galerkin approach using a basis of trigonometric functions. However this method is designed to approximate periodic solutions with known period (Cameron and Griffin, 1989; von Groll and Ewins, 2001). Briefly, the time vector $\mathbf{q}(t)$ is developed in a truncated Fourier series:

$$\mathbf{q}(t) = \frac{\mathbf{a}_0}{\sqrt{2}} + \sum_{k=1}^{K} \left(\mathbf{a}_k \cos(k\omega t) + \mathbf{b}_k \sin(k\omega t) \right) \tag{15}$$

where coefficients $\mathbf{a}_k$ and $\mathbf{b}_k$ are real vectors with same size as $\mathbf{q}$, and $\omega = 2\pi/T$ is the limit cycle angular frequency. This development imposes $\dot{\mathbf{q}}$ and

$\ddot{\mathbf{q}}$ as well.

Once reinjected in the dynamical equation, the time variable is eliminated by projecting the system of equations onto the functions $1/\sqrt{2}$, $\cos(k\omega t)$ and $\sin(k\omega t)$ using the scalar product

$$< f, g >= \frac{2}{T}\int_{t=0}^{T} f(t)g(t)dt \tag{16}$$

If $\mathbf{q}$ size is n, this generates a square system of equations with size $n(2K+1)$.

Yet, when angular frequency ω is unknown, the system is not square anymore and one usually wishes to add an equation or remove an unknown. Work presented in (Coudeyras et al., 2009) explores the first solution by adding a constraint on real parts of eigenvalues of the tangent system. This procedure requires a lot of computation and does not fit further developments when uncertainties is introduced. Therefore, this study proposes to explore the second solution which consists in removing an unknown by setting it to a given value as suggested in (Seydel, 1988). It will be referred to as CHBM for Constrained Harmonic Balance Method. It is an interesting improvement of usual HBM procedure that provides a way to catch limit cycles of self-excited non-linear systems which is hardly treated in the literature.

For the current system, $\mathbf{q}(t)$ is developed with only one harmonic and no constant term (for centred solutions approximation only); an unknown is removed by assigning a given value a_1^* to the first component of $\mathbf{a}$ vector:

$$\mathbf{q}(t) = \mathbf{a}\cos(\omega t) + \mathbf{b}\sin(\omega t),\ \mathbf{a} = \left\{ \begin{array}{c} a_1^* \\ a_2 \end{array} \right\}, \mathbf{b} = \left\{ \begin{array}{c} b_1 \\ b_2 \end{array} \right\} \tag{17}$$

Injecting this decomposition in the dynamic equation (1) and projecting the resulting set of equations onto $\cos(\omega t)$ and $\sin(\omega t)$ functions using scalar

product (16), one finally gets the algebraic set

$$\left(\mathbf{K}-\omega^2\mathbf{M}\right)\mathbf{a}+\omega\mathbf{D}\mathbf{b}+\frac{3}{4}\begin{Bmatrix}(a_1^{*3}+a_1^*b_1^2)\varphi_1-(a_2^3+a_2b_2^2)\mu\varphi_2\\(a_1^{*3}+a_1^*b_1^2)\mu\varphi_1+(a_2^3+a_2b_2^2)\varphi_2\end{Bmatrix}=\mathbf{0} \quad (18a)$$

$$\left(\mathbf{K}-\omega^2\mathbf{M}\right)\mathbf{b}-\omega\mathbf{D}\mathbf{a}+\frac{3}{4}\begin{Bmatrix}(a_1^{*2}b_1+b_1^3)\varphi_1-(a_2^2b_2+b_2^3)\mu\varphi_2\\(a_1^{*2}b_1+b_1^3)\mu\varphi_1+(a_2^2b_2+b_2^3)\varphi_2\end{Bmatrix}=\mathbf{0} \quad (18b)$$

where the four unknowns are a_2, b_1, b_2 and ω.

3.2.2. Stochastic case

When some parameters are uncertain, the limit cycles are affected too. Dispersion is then approximated using an expansion of CHBM unknowns on the polynomial chaos:

$$\begin{aligned}\tilde{a}_2(\boldsymbol{\xi})&=\sum_{n=1}^{N'}\alpha_2^n\psi_n(\boldsymbol{\xi})\,,\ \tilde{b}_1(\boldsymbol{\xi})=\sum_{n=1}^{N'}\beta_1^n\psi_n(\boldsymbol{\xi}),\\ \tilde{\omega}(\boldsymbol{\xi})&=\sum_{n=1}^{N'}\varpi^n\psi_n(\boldsymbol{\xi}),\ \tilde{b}_2(\boldsymbol{\xi})=\sum_{n=1}^{N'}\beta_2^n\psi_n(\boldsymbol{\xi}),\end{aligned} \quad (19)$$

where decomposition coefficients α_2^n, β_1^n, β_2^n and ϖ^n are real.

These approximations are injected into the CHBM deterministic equations (18) where uncertainty on matrices and non-linear function have been introduced. For example, for the third uncertain configuration processed in Section 4.2 (i.e. uncertainties for the friction coefficient μ and the damping

ratio η_2), one gets

$$\begin{aligned}
&\Big((\mathbf{K}+\tilde{\mathbf{K}}(\boldsymbol{\xi}))-\tilde{\omega}^2(\boldsymbol{\xi})\mathbf{M}\Big)\begin{Bmatrix} a_1^* \\ \tilde{a}_2(\boldsymbol{\xi})\end{Bmatrix} \\
&\quad+\tilde{\omega}(\boldsymbol{\xi})(\mathbf{D}+\tilde{\mathbf{D}}(\boldsymbol{\xi}))\begin{Bmatrix}\tilde{b}_1(\boldsymbol{\xi}) \\ \tilde{b}_2(\boldsymbol{\xi})\end{Bmatrix} \\
&\quad+\frac{3}{4}\begin{Bmatrix}(a_1^{*3}+a_1^*\tilde{b}_1^2(\boldsymbol{\xi}))\varphi_1-(\tilde{a}_2^3(\boldsymbol{\xi})+\tilde{a}_2(\boldsymbol{\xi})\tilde{b}_2^2(\boldsymbol{\xi}))(\overline{\mu}+\xi_1\Delta\mu)\varphi_2 \\ (a_1^{*3}+a_1^*\tilde{b}_1^2(\boldsymbol{\xi}))(\overline{\mu}+\xi_1\Delta\mu)\varphi_1+(\tilde{a}_2^3(\boldsymbol{\xi})+\tilde{a}_2(\boldsymbol{\xi})\tilde{b}_2^2(\boldsymbol{\xi}))\varphi_2\end{Bmatrix} \\
&\quad=\mathbf{0}
\end{aligned} \tag{20a}$$

$$\begin{aligned}
&\Big((\mathbf{K}+\tilde{\mathbf{K}}(\boldsymbol{\xi}))-\tilde{\omega}^2(\boldsymbol{\xi})\mathbf{M}\Big)\begin{Bmatrix}\tilde{b}_1(\boldsymbol{\xi}) \\ \tilde{b}_2(\boldsymbol{\xi})\end{Bmatrix} \\
&\quad-\tilde{\omega}(\boldsymbol{\xi})(\mathbf{D}+\tilde{\mathbf{D}}(\boldsymbol{\xi}))\begin{Bmatrix} a_1^* \\ \tilde{a}_2(\boldsymbol{\xi})\end{Bmatrix} \\
&\quad+\frac{3}{4}\begin{Bmatrix}(a_1^{*2}\tilde{b}_1(\boldsymbol{\xi})+\tilde{b}_1^3(\boldsymbol{\xi}))\varphi_1-(\tilde{a}_2^2(\boldsymbol{\xi})\tilde{b}_2(\boldsymbol{\xi})+\tilde{b}_2^3(\boldsymbol{\xi}))(\overline{\mu}+\xi_1\Delta\mu)\varphi_2 \\ (a_1^{*2}\tilde{b}_1(\boldsymbol{\xi})+\tilde{b}_1^3(\boldsymbol{\xi}))(\overline{\mu}+\xi_1\Delta\mu)\varphi_1+(\tilde{a}_2^2(\boldsymbol{\xi})\tilde{b}_2(\boldsymbol{\xi})+\tilde{b}_2^3(\boldsymbol{\xi}))\varphi_2\end{Bmatrix} \\
&\quad=\mathbf{0}
\end{aligned} \tag{20b}$$

with

$$\tilde{\mathbf{K}}(\boldsymbol{\xi})=\xi_1\Delta\mu\begin{bmatrix}0 & -\omega_{02}^2 \\ \omega_{01}^2 & 0\end{bmatrix} \tag{21a}$$

$$\tilde{\mathbf{D}}(\boldsymbol{\xi})=\xi_2\Delta\eta_2\begin{bmatrix}0 & 0 \\ 0 & \omega_{02}\end{bmatrix} \tag{21b}$$

The final set of $4N'$ equations is obtained by projecting this system onto the Hermite polynomials ψ_n, $1\leq n\leq N'$ using the associate scalar product (A.5). The final system of equations providing the decomposition of CHBM coefficients on PC is non-linear and solved using an appropriate algorithm.

4. Results and Discussion

This part is dedicated to application of the methods exposed in the previous section. Each of the three proposed cases permits the illustration of different physical phenomena and is a support for showing suitability of the approaches for accurate stochastic studies.

4.1. Case 1: dispersion on friction coefficient μ - Stability analysis

Variation of the friction coefficient μ has effect on the static equilibrium stability. Therefore, focus is put on accuracy of eigenvalues and especially their real part. First, PC coefficients are evaluated for different orders D of expansion, namely $1 \leq D \leq 3$. Having only one random variable ξ, the PC basis used consists in $N = D + 1$ polynomials ψ_n, $1 \leq n \leq N$ where $\psi_1(\xi) = 1$, $\psi_2(\xi) = \xi$, $\psi_3(\xi) = \xi^2 - 1$ and $\psi_4(\xi) = \xi^3 - 3\xi$. Then a set of 10000 sample points $\xi^{(j)}$ is generated (using a standard normal distribution) and used to evaluate $\tilde{\lambda}_k(\xi^{(j)})$, $1 \leq k \leq 4$, $1 \leq j \leq 10000$ using the different PC approximations as well as direct Monte Carlo computation. This last set of values is considered as the reference set. Note that is has been verified that μ values resulting from this sample made physical sense.

Results are showed on Fig. 2. On this figure, only eigenvalues with positive imaginary part are displayed, others being directly complex conjugate. The left panes are devoted to the imaginary parts and the right ones to the real parts. Fig. 2 (a) displays Monte Carlo simulations results while the three lower blocks (b) to (d) display histograms of absolute relative error computed as follow for relative error on imaginary part

$$\mathrm{e}_{\mathrm{rel}} = \frac{\left|\mathrm{Im}\left(\lambda^{\mathrm{PC}}\right) - \mathrm{Im}\left(\lambda^{\mathrm{MC}}\right)\right|}{\left|\mathrm{Im}\left(\lambda^{\mathrm{MC}}\right)\right|} \times 100 \tag{22}$$

	MC	PCE order 1	PCE order 2	PCE order 3
Stable	5187	4705	5185	5213
Unstable	4813	5295	4815	4787

Table 1: Uncertain μ: comparison of PC expansion (PCE) results with MC simulation (stable occurrences counts)

and in an equivalent way for real parts. MC and PC superscripts denote values obtained using direct Monte Carlo and PC expansion evaluation respectively. This error is computed for each mode (1 and 2) and each point $\xi^{(j)}$ of the sample, leading to the proposed histograms.
One can see that error on imaginary part is almost negligible whatever the PC order is. On the contrary, the real part of eigenvalue for mode 1 really takes advantage on the higher orders. Finally, order $D = 3$ gives accurate enough results with an error mostly lower than 5 percent.

Moreover, these eigenvalues being mainly used to predict the stability of the equilibrium, the number of stable and unstable occurrences is summed up in Table 1. Once again, order 2 and order 3 PC expansions reproduce these counts with very little difference to the Monte Carlo reference.

This comparison shows that even for great dispersion of the input value (standard deviation being 5 % of the nominal value with a Gaussian repartition, it means that 99% of the values are within a range with width equal to 30% of the nominal value), the PC expansion method suits representation of eigenvalues dispersion and so the system stability and instability rate with a satisfying accuracy.

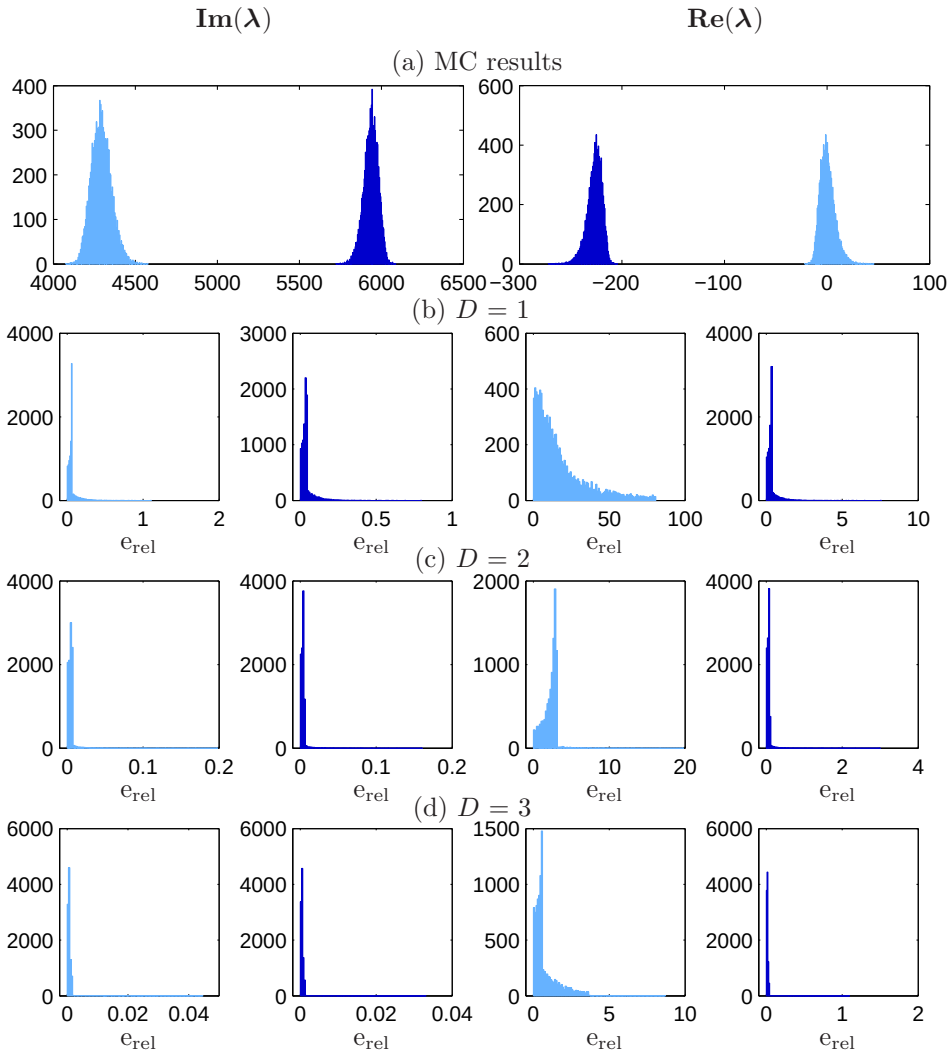

Figure 2: Uncertain μ: comparison of PC expansion results with MC simulations. Left half: quantities relative to imaginary part of eigenvalues. Right half: quantities relative to real part of eigenvalues. (a) MC simulations; (b) to (d) histograms of absolute relative error (in percent) between PC and MC results for each mode and different PC orders D. Light blue: mode 1; dark blue: mode 2.

4.2. Case 2: dispersion on damping ratio η_2 - Limit cycles study

The aim of this configuration being to monitor η_2 influence on the mode becoming unstable and the subsequent limit cycles, the friction coefficient μ is chosen great enough to ensure unstable equilibria whatever η_2 value may be.

First, eigenmodes PC expansion coefficients were evaluated using an order 3 decomposition. Then a sample of 10000 points was used to evaluate eigenvalues. Results are presented in Fig. 3. They confirm that the instability may come from either mode 1 or mode 2 depending on the value of η_2.

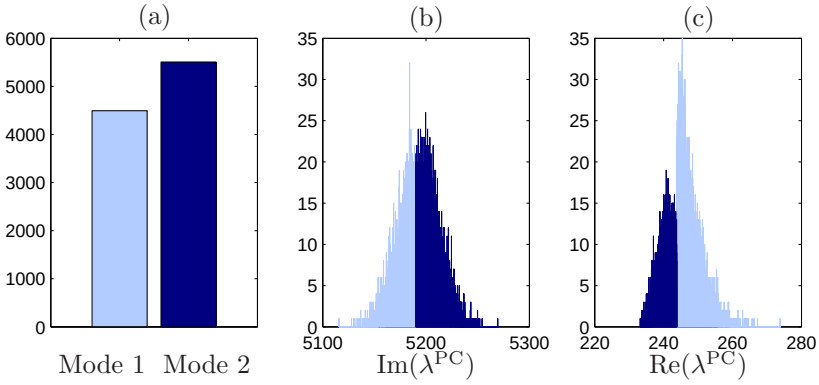

Figure 3: Uncertain η_2: unstable mode histograms. (a) Unstable mode number; (b) Imaginary part and (c) Real part of unstable eigenvalue. Light blue: mode 1, dark blue: mode 2

In a second time, stress is put on the limit cycles. Their dispersion is evaluated using the CHBM method exposed in Section 3.2 using $a_1^* = 2 \cdot 10^{-3}$. Different orders for PC expansion are tested and compared to deterministic results for 11 points $\xi^{(j)}$ equally spaced between -3 and $+3$. For each variable a_2, b_1, b_2 and ω, the absolute relative error between the value obtained using PC expansion and the one obtained using direct calculation is evalu-

ated. Results are summed up in Fig. 4. This shows that order 3 and order 4 expansions give very accurate results. The deterministic results were previously checked using them as initial conditions for a time integration with duration $T = 2\pi/\omega$ for each of the 11 test points and verifying that initial and final states were almost identical. Order 4 PC expansion is retained for

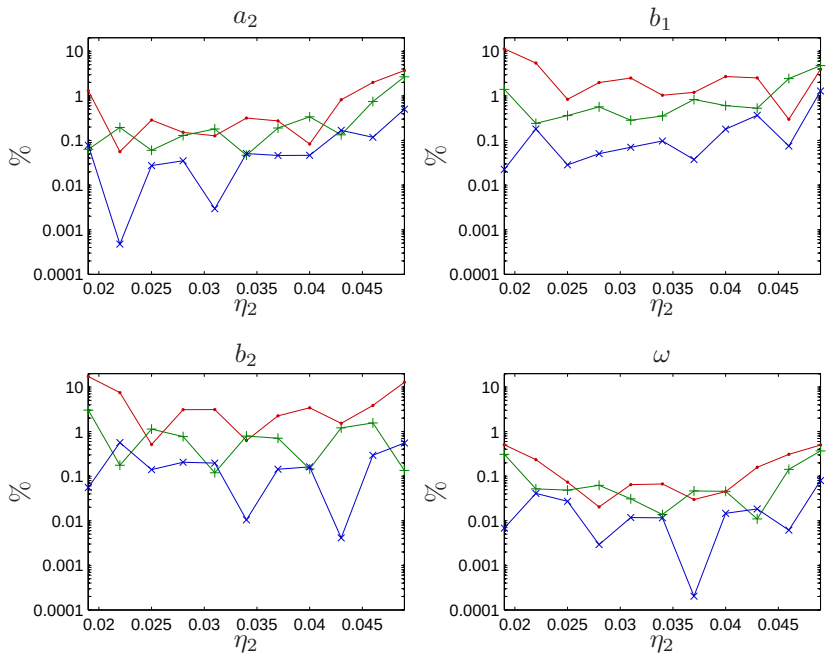

Figure 4: Uncertain η_2: CHBM PCE results comparison with deterministic results for different PC expansion orders using absolute relative error in percent.
–·–: order $D = 2$; –+–: order $D = 3$; –×–: order $D = 4$.

comparison with MC simulation on a larger sample. Fig. 5 exposes the results of this comparison by showing MC simulation results for each variable a_2, b_1, b_2 and ω as well as the absolute relative error (in percent) between PC expansion and MC simulation. This confirms that error is mostly lower than 1 % for each variable and hence that PC expansion is an accurate method

to describe stochastic CHBM coefficients. Moreover, direct computation for a sample with 10000 points required 190 s while PC method only used 0.60 s for evaluation of PC expansion of coefficients and 0.24 s for evaluation of the 10000 realizations: direct MC simulation is about 226 times longer than the proposed method.

Finally, PC expansion with order 4 is used to rebuild cycles over time to visually check occupation rate in different spaces as depicted on Fig. 6. The procedure used to build these portraits is the following: for each point $\xi^{(j)}$, $\mathbf{q}$ and $\dot{\mathbf{q}}$ vectors are evaluated at 1000 time points $\tau_k = 2\pi/1000 \times (k-1)$ using formula:

$$\mathbf{q}_k^{(j)} = \begin{Bmatrix} a_1^* \\ \tilde{a}_2(\xi^{(j)}) \end{Bmatrix} \cos(\tau_k) + \begin{Bmatrix} \tilde{b}_1(\xi^{(j)}) \\ \tilde{b}_2(\xi^{(j)}) \end{Bmatrix} \sin(\tau_k) \tag{23a}$$

$$\dot{\mathbf{q}}_k^{(j)} = \omega(\xi^{(j)}) \left(- \begin{Bmatrix} a_1^* \\ \tilde{a}_2(\xi^{(j)}) \end{Bmatrix} \sin(\tau_k) + \begin{Bmatrix} \tilde{b}_1(\xi^{(j)}) \\ \tilde{b}_2(\xi^{(j)}) \end{Bmatrix} \cos(\tau_k) \right) \tag{23b}$$

Then, to build (q_1, q_2) portrait for example, minimum and maximum values for each variable are evaluated and a grid is used with 251 bins in each direction to divide (q_1, q_2) space. For each cycle $\mathbf{q}_k^{(j)}$, $1 \leq k \leq 1000$, $\mathbf{q}_k^{(j)}$ at time τ_k is located in the grid. If it is located in the same bin as the previous time point $\mathbf{q}_{k-1}^{(j)}$, it is not counted; otherwise, +1 is added to the bin weight. This avoids affecting too much weight to a bin because of high time discretization. When all the cycles are processed, the weights are divided by the number of cycles (10000) and multiplied by 100: this gives for each grid point a percentage of occupation.

As can be seen on Fig. 6 (a), two modes can contribute when the equilibrium is unstable resulting in two different main orientations for the cycles.

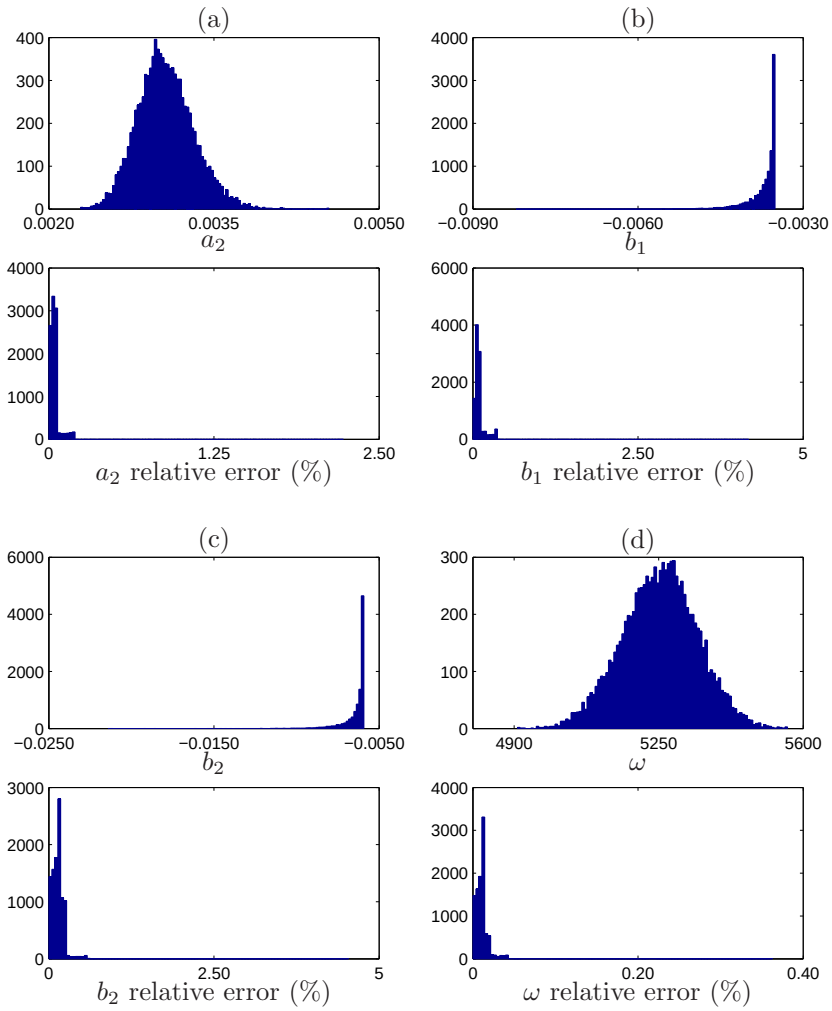

Figure 5: Uncertain η_2: CHBM order 4 PC expansion results comparison with MC deterministic results. MC results and absolute relative error (in percent) for (a) a_2, (b) b_1, (c) b_2 and (d) ω coefficients.

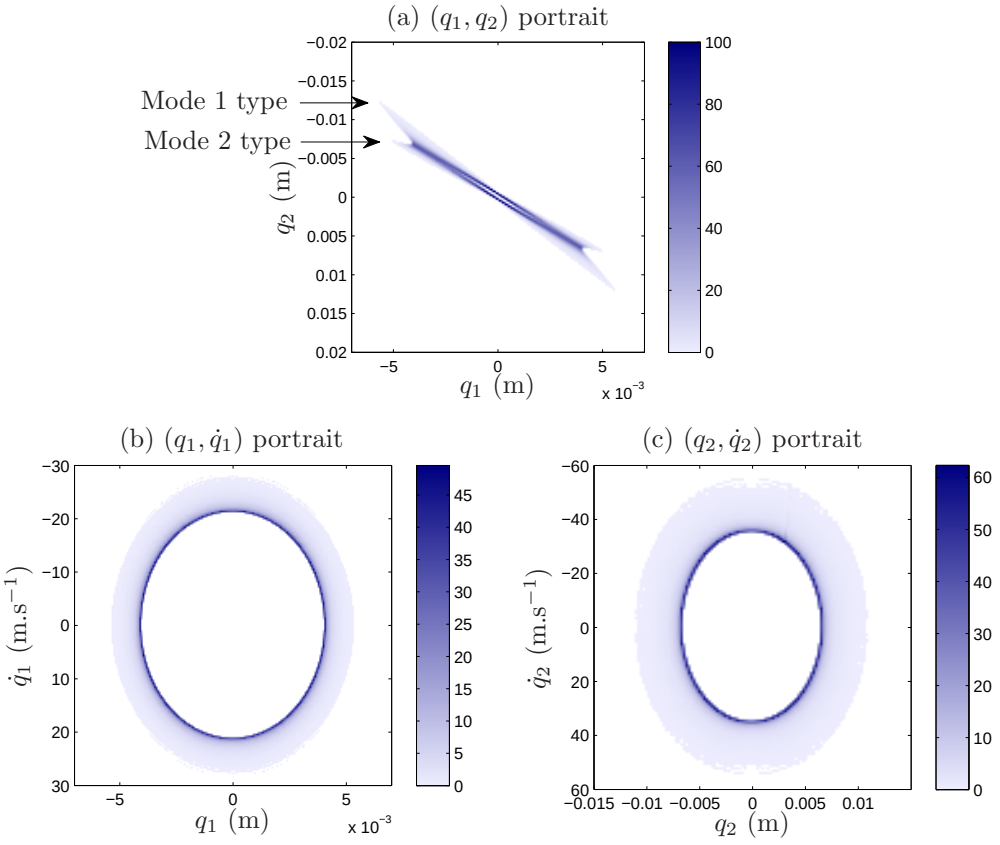

Figure 6: Uncertain η_2: dispersion in different spaces rebuilt from PC expansion with order 4.

4.3. Case 3: dispersion on both variables μ and η_2

For this last configuration, two independent random variables are used. First, eigenvalues are decomposed on PC using an order 2 expansion. This involves the following polynomials: $\psi_1(\boldsymbol{\xi}) = 1$, $\psi_2(\boldsymbol{\xi}) = \xi_1$, $\psi_3(\boldsymbol{\xi}) = \xi_2$, $\psi_4(\boldsymbol{\xi}) = \xi_1^2 - 1$, $\psi_5(\boldsymbol{\xi}) = \xi_1\xi_2$ and $\psi_6(\boldsymbol{\xi}) = \xi_2^2 - 1$. Using the random sample of 10000 points represented in Fig. 7 (a), one can rebuild the eigenvalues and plot the location probability (in percent) of the unstable eigenvalue in the complex plane. It is also possible to distinguish between the occurrences for which mode number 1 becomes unstable and the ones for which instability comes from mode number 2 (Fig. 7 (b) and (c)). It turns out that for this configuration, all the occurrences are relative to an unstable equilibrium. Among the 10000 points, 5375 become unstable because of mode 1 and 4625 because of mode 2.

After the stability study, the limit cycles were fitted using an order 2 PC expansion. Using the same procedure as the one described previously, one can draw portraits in different spaces as depicted in Fig. 8. This time, dispersion being smaller than in the second case, one cannot clearly identify very different behaviours because mode 1 and mode 2 keep being very close from one another.

5. Conclusions

Two methods designed for stochastic study of systems with friction were exposed. The first one provides a way to evaluate complex eigenmodes dispersion by using an expansion of stochastic eigenmodes on both the deterministic eigenmodes and the Polynomial Chaos. The second method evaluates

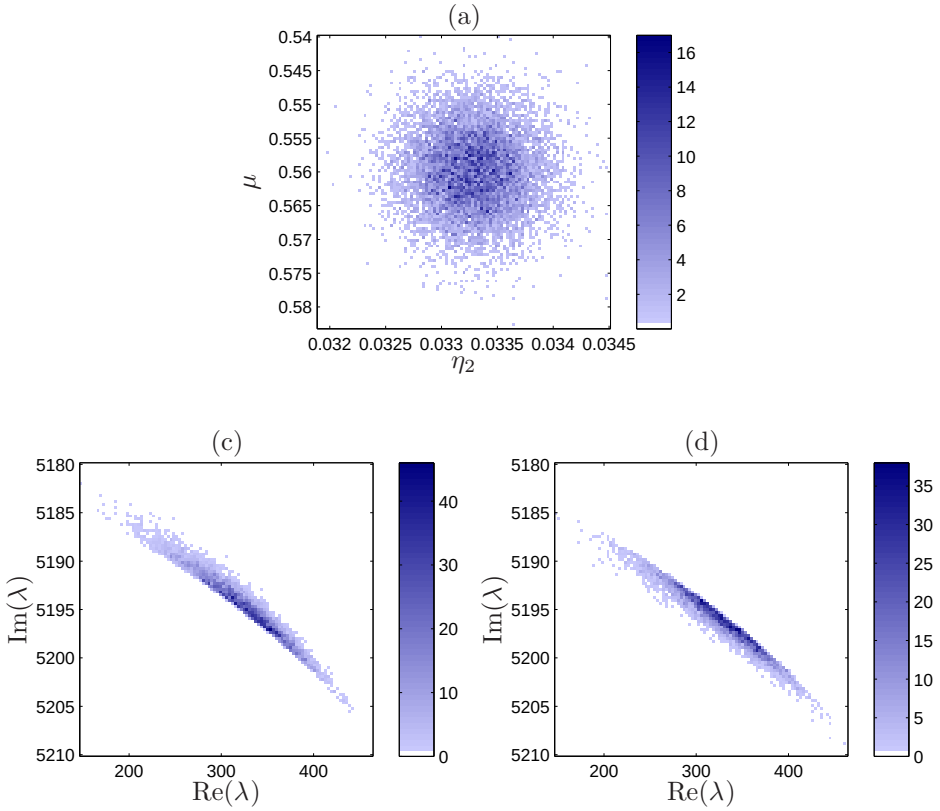

Figure 7: Uncertain η_2 and μ: unstable mode dispersion; (a) Random sample; (b) Unstable mode 1 and (c) unstable mode 2 eigenvalue in complex plane

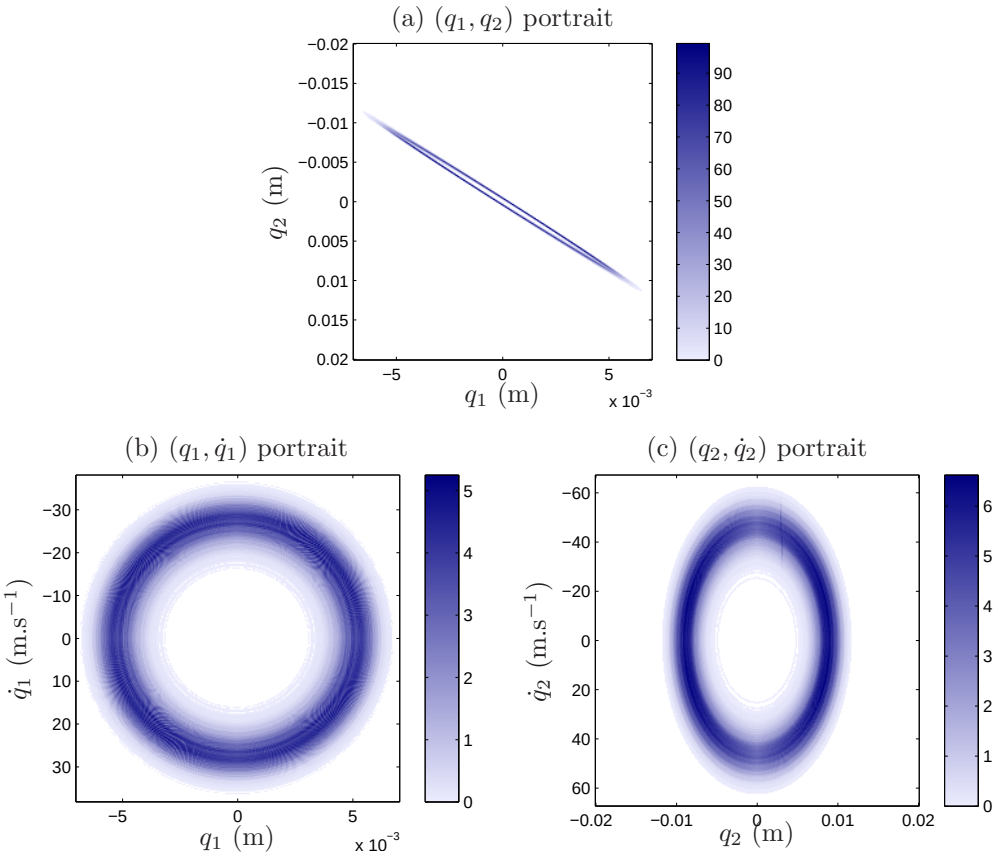

Figure 8: Uncertain η_2 and μ: dispersion in different spaces rebuilt from PC expansion with order 4.

dispersion on limit cycles amplitudes and frequencies. It can been seen as an improvement of the usual HBM combined with a constraint that provides a way to deal with limit cycles having an unknown period and a Polynomial Chaos expansion of its coefficients.

Through three uncertain configurations, they were demonstrated to be accurate and efficient, using comparison with direct calculation, even in the case of wide uncertainty ranges.

A. Hermite multivariate polynomials

Hermite polynomials (one dimension) can be defined using a derivative

$$h_n(\xi) = (-1)^n \mathrm{e}^{\xi^2/2} \frac{\mathrm{d}^\mathrm{n} \mathrm{e}^{-\xi^2/2}}{\mathrm{d}\xi^\mathrm{n}} \tag{A.1}$$

or recursively (formula from (Sudret and Der Kiureghian, 2000, Section 3.2)):

$$h_0(\xi) = 1 \tag{A.2a}$$

$$\frac{dh_n(\xi)}{d\xi} = n h_{n-1}(\xi) \tag{A.2b}$$

$$h_n(0) = \begin{cases} 0 & \text{if } n \text{ is odd} \\ (-1)^{n/2} \dfrac{n!}{2^{n/2}(\frac{n}{2})!} & \text{if } n \text{ is even} \end{cases} \tag{A.2c}$$

The general formula for multidimensional Hermite polynomials is

$$\psi_m(\xi_{i_1}, \ldots, \xi_{i_n}) = (-1)^n \mathrm{e}^{\frac{1}{2}\boldsymbol{\xi}^\mathrm{T}\boldsymbol{\xi}} \frac{\partial^\mathrm{n} \mathrm{e}^{-\frac{1}{2}\boldsymbol{\xi}^\mathrm{T}\boldsymbol{\xi}}}{\partial\xi_{\mathrm{i}_1} \ldots \partial\xi_{\mathrm{i}_\mathrm{n}}} \tag{A.3}$$

but the formula used in practice to compute the multivariate Hermite polynomials is the one found in (Sudret and Der Kiureghian, 2000, Chap. 3,

Section 3.1): for Q random variables, the multivariate Hermite polynomials of order d can be expressed as

$$\psi_\alpha = \prod_{i=1}^{Q} h_{\alpha_i}(\xi_i) \tag{A.4}$$

with $\alpha = (\alpha_1, \ldots, \alpha_Q) \in \{0, \ldots, d\}^Q$ such that $\sum_{i=1}^{Q} \alpha_i = d$.
There are exactly

$$\frac{(d+Q-1)!}{d!(Q-1)!}$$

polynomials with degree d. That is, for Q random variables, there are N polynomials with degree less than or equal to D:

$$N = \frac{(D+Q)!}{D!Q!}$$

These polynomials are orthogonal with respect to the following scalar product

$$< f, g >= \frac{1}{\sqrt{2\pi}^Q} \int_{\xi_1=-\infty}^{+\infty} \ldots \int_{\xi_Q=-\infty}^{+\infty} f(\xi_1, \ldots, \xi_Q) \times g(\xi_1, \ldots, \xi_Q) e^{-\boldsymbol{\xi}^{\mathrm{T}}\boldsymbol{\xi}/2} d\xi_1 \ldots d\xi_Q \tag{A.5}$$

Acknowledgements

The authors gratefully acknowledge the financial support of the French National Research Agency through the Young Researcher program ANR-07-JCJC-0059-01-CSD2.

References

Butlin, T., Woodhouse, J., 2009. Friction-induced vibration: Should low-order models be believed? Journal of Sound and Vibration 328, 92 – 108.

Butlin, T., Woodhouse, J., 2010. Friction-induced vibration: Quantifying sensitivity and uncertainty. Journal of Sound and Vibration 329, 509 – 526.

Cameron, T.M., Griffin, J.H., 1989. An alternating frequency/time domain method for calculating the steady-state response of nonlinear dynamic systems. Journal of Applied Mechanics 56, 149–154.

Coudeyras, N., Sinou, J.J., Nacivet, S., 2009. A new treatment for predicting the self-excited vibrations of nonlinear systems with frictional interfaces: The constrained harmonic balance method, with application to disc brake squeal. Journal of Sound and Vibration 319, 1175 – 1199.

Dessombz, O., 2000. Analyse dynamique de structures comportant des paramètres incertains (Dynamic analysis of structures with uncertain parameters). Ph.D. thesis. Ecole Centrale de Lyon/MEGA.

Dessombz, O., Diniz, A., Thouverez, F., , Jézéquel, L., 1999. Analysis of stochastic structures: perturbation method and projection on homogeneous chaos, in: Proceedings of the IMAC XVII, Kissimmee, FL, USA. pp. 1763–1769.

Fisher, J., Bhattacharya, R., 2008. Stability analysis of stochastic systems

using polynomial chaos, in: 2008 American Control Conference, Westin Seatle Hotel, Seatle, Washington, USA. pp. 4250–4255. June 11-13.

Ghanem, R., Spanos, P., 2003. Stochastic finite elements: a spectral approach - Revised Edition. Dover Publications.

von Groll, G., Ewins, D.J., 2001. The harmonic balance method with arclength continuation in rotor/stator contact problems. Journal of Sound and Vibration 241, 223–233.

Hultén, J., 1993. Drum brake squeal – a self-exciting mechanism with constant friction, in: SAE Truck and Bus Meeting, Detroit, Mi, USA. SAE Paper 932965.

Ibrahim, R.A., 1994. Friction-induced vibration, chatter, squeal, and chaos—part i: Mechanics of contact and friction. Applied Mechanics Reviews 47, 209–226.

Kinkaid, N.M., O'Reilly, O.M., Papadopoulos, P., 2003. Automotive disc brake squeal. Journal of Sound and Vibration 267, 105 – 166.

Nechak, L., Berger, S., Aubry, E., 2011. A polynomial chaos approach to the robust analysis of the dynamic behaviour of friction systems. European Journal of Mechanics - A/Solids 30, 594–607.

Nechak, L., Berger, S., Aubry, E., 2012. Prediction of random self friction-induced vibrations in uncertain dry friction systems using a multi-element generalized polynomial chaos approach. Journal of Vibration and Acoustics 134, 041015.

Nechak, L., Berger, S., Aubry, E., 2013. Non-intrusive generalized polynomial chaos for the robust stability analysis of uncertain nonlinear dynamic friction systems. Journal of Sound and Vibration In press.

Sarrouy, E., Dessombz, O., Sinou, J.J., 2013. Piecewise polynomial chaos expansion with an application to brake squeal of a linear brake system. Journal of Sound and Vibration 332, 577–594.

Seydel, R., 1988. From Equilibrium to Chaos, Practical Bifurcation and Stability Analysis. Elsevier.

Sinou, J.J., Jézéquel, L., 2007a. The influence of damping on the limit cycles for a self-exciting mechanism. Journal of Sound and Vibration 304, 875 – 893.

Sinou, J.J., Jézéquel, L., 2007b. Mode coupling instability in friction-induced vibrations and its dependency on system parameters including damping. European Journal of Mechanics - A/Solids 26, 106 – 122.

Sudret, B., Der Kiureghian, A., 2000. Stochastic Finite Element Methods and Reliability: A State-of-the-Art Report. Technical Report. University of California, Berkeley.

Wan, X., Karniadakis, G.E., 2005. An adaptive multi-element generalized polynomial chaos method for stochastic differential equations. Journal of Computational Physics 209, 617 – 642.